Molecular and Cellular Biology

Targeted Disruption of the Idol Gene Alters Cellular Regulation of the Low-Density Lipoprotein Receptor by Sterols and Liver X Receptor Agonists

Elena Scotti, Cynthia Hong, Yuko Yoshinaga, Yiping Tu, Yan Hu, Noam Zelcer, Rima Boyadjian, Pieter J. de Jong, Stephen G. Young, Loren G. Fong and Peter Tontonoz

Mol. Cell. Biol. **2011, 31(9):1885. DOI: 10.1128/MCB.01469-10.**
Published Ahead of Print 22 February 2011.

MOLECULAR AND CELLULAR BIOLOGY, May 2011, p. 1885–1893 Vol. 31, No. 9
0270-7306/11/$12.00 doi:10.1128/MCB.01469-10

Targeted Disruption of the Idol Gene Alters Cellular Regulation of the Low-Density Lipoprotein Receptor by Sterols and Liver X Receptor Agonists▽§

Elena Scotti,[1,2,6] Cynthia Hong,[1,2] Yuko Yoshinaga,[5] Yiping Tu,[4] Yan Hu,[4] Noam Zelcer,[1,2]† Rima Boyadjian,[1,2] Pieter J. de Jong,[5] Stephen G. Young,[3,4] Loren G. Fong,[4] and Peter Tontonoz[1,2]*

Howard Hughes Medical Institute,[1] Department of Pathology and Laboratory Medicine,[2] Department of Human Genetics,[3] and Department of Medicine,[4] University of California, Los Angeles, Los Angeles, California; Children's Hospital of Oakland Research Institute, Oakland, California[5]; and Dipartimento di Scienze Farmacologiche, Università degli Studi di Milano, Milan, Italy[6]

Received 27 December 2010/Returned for modification 29 January 2011/Accepted 12 February 2011

Previously, we identified the E3 ubiquitin ligase Idol (inducible degrader of the low-density lipoprotein [LDL] receptor [LDLR]) as a posttranscriptional regulator of the LDLR pathway. Idol stimulates LDLR degradation through ubiquitination of its C-terminal domain, thereby limiting cholesterol uptake. Here we report the generation and characterization of mouse embryonic stem cells homozygous for a null mutation in the Idol gene. Cells lacking Idol exhibit markedly elevated levels of the LDLR protein and increased rates of LDL uptake. Furthermore, despite an intact sterol responsive element-binding protein (SREBP) pathway, Idol-null cells exhibit an altered response to multiple regulators of sterol metabolism, including serum, oxysterols, and synthetic liver X receptor (LXR) agonists. The ability of oxysterols and lipoprotein-containing serum to suppress LDLR protein levels is reduced, and the time course of suppression is delayed, in cells lacking Idol. LXR ligands have no effect on LDLR levels in Idol-null cells, indicating that Idol is required for LXR-dependent inhibition of the LDLR pathway. In line with these results, the half-life of the LDLR protein is prolonged in the absence of Idol. Finally, the ability of statins and PCSK9 to alter LDLR levels is independent of, and additive with, the LXR-Idol pathway. These results demonstrate that the LXR-Idol pathway is an important contributor to feedback inhibition of the LDLR by sterols and a biological determinant of cellular LDL uptake.

Cholesterol plays key roles in biological systems, including developmental signaling, control of membrane fluidity, and formation of caveolae (3). However, free cholesterol can be harmful in excess, and for this reason its levels must be tightly regulated. Whole-body cholesterol homeostasis reflects a balance between endogenous synthesis, dietary uptake, and biliary excretion. Two major transcriptional regulatory pathways have evolved in mammals to coordinate responses to both elevated and reduced cellular cholesterol content: the sterol responsive element-binding proteins (SREBPs) and the liver X receptors (LXRs). These transcription factors regulate gene expression in a tissue-specific fashion to maintain both whole-body and cellular sterol homeostasis.

The response to low intracellular cholesterol content is mediated primarily by the transcription factor SREBP-2. The precursor protein resides in the endoplasmic reticulum (ER) and is transported to the Golgi apparatus under sterol-poor conditions, where it undergoes proteolytic processing. The mature SREBP protein translocates to the nucleus and switches on the transcription of sterol biosynthetic genes, including 3-hydroxy-3-methyl-glutaryl-coenzyme A (CoA) reductase (HMGCoAR) and 3-hydroxy-3-methyl-glutaryl-CoA synthase (HMGCoA synthase). In addition, SREBP promotes the expression of the low-density lipoprotein receptor (LDLR), thereby increasing LDL uptake and cholesterol delivery to cells (7). SREBPs also control the expression of proprotein convertase subtilisin/kexin type 9 (PCSK9), a protein involved in the posttranscriptional regulation of the LDLR (15, 24). PCSK9 binds directly to the extracellular domain of the LDLR and alters its stability and trafficking, thereby increasing degradation in lysosomes (5, 15, 28). SREBP-mediated regulation of PCSK9 and its consequent downregulation of the LDLR have been proposed as a mechanism to prevent reuptake of newly secreted very low density lipoprotein (VLDL) particles by hepatocytes, thereby shunting them toward peripheral tissues (8).

On the other hand, the nuclear receptor superfamily members LXRα and LXRβ respond to excess cholesterol. Oxysterols, products of enzymatic or nonenzymatic cholesterol oxidation, are formed when cellular cholesterol rises and serve as ligands for LXRs (10). 24,25-Expoxycholesterol and 22(*R*)-hydroxycholesterol are particularly potent and efficacious LXR ligands (11). Activation of LXR by oxysterols induces the expression of genes involved in cholesterol efflux from cells, including ATP-binding cassette transporter G1 (ABCG1),

* Corresponding author. Mailing address: Howard Hughes Medical Institute, UCLA School of Medicine, Box 951662, Los Angeles, CA 90095-1662. Phone: (310) 206-4546. Fax: (310) 267-0382. E-mail: ptontonoz@mednet.ucla.edu.

† Present address: Department of Medical Biochemistry, Academic Medical Center, University of Amsterdam, Amsterdam, Netherlands.

▽ Published ahead of print on 22 February 2011.

§ The authors have paid a fee to allow immediate free access to this article.

ABCA1, and apolipoprotein E (apoE) (6, 12, 21, 25). Thus, LXR activation promotes the transfer of excess cholesterol to extracellular acceptors, such as apolipoprotein A1 and high-density lipoproteins (HDL).

Another mechanism by which LXR modulates cholesterol homeostasis is through the transcriptional induction of the E3 ubiquitin ligase Idol (inducible degrader of the LDL receptor). We showed that Idol triggers ubiquitination of the LDLR on its cytoplasmic domain, thereby targeting it for degradation. LXR agonists reduce LDLR protein levels in a cell- and tissue-specific manner, and adenovirus-driven expression of Idol in mouse liver raises plasma LDL levels (27). More recently, we reported that Idol can induce the degradation of two other LDLR family members, apoE receptor 2 (apoER2) and the very low density lipoprotein receptor (VLDLR) (9). The consequences of a genetic deficiency of Idol for cellular cholesterol homeostasis and LDLR regulation have not been addressed previously.

Here we report the generation and characterization of mouse embryonic stem (ES) cells homozygous for a null mutation in the Idol gene. Our results show that endogenous Idol expression is an important determinant of LDLR protein levels and LDL uptake and that Idol is required for maximal feedback inhibition of the LDLR by sterols. Furthermore, we demonstrate that Idol expression is required for the ability of LXR to stimulate LDLR protein degradation. Finally, we provide evidence that Idol, PCSK9, and SREBP represent independent but complementary mechanisms for regulation of LDLR protein levels.

MATERIALS AND METHODS

Reagents. GW3965 was provided by T. Wilson and J. Collins (GlaxoSmithKline). Mevalonic acid, 22(*R*)-hydroxycholesterol, and 25-hydroxycholesterol were from Sigma-Aldrich. Simvastatin sodium salt was from Calbiochem. DiI-LDL was purchased from Molecular Probes, and lipoprotein-deficient fetal bovine serum (LPDS) was purchased from Intracell. Purified PCSK9 was kindly provided by Helen Hobbs (University of Texas Southwestern, Dallas, TX).

Idol conditional knockout targeting vector. A bacterial artificial chromosome (BAC) clone, clone RP23-473O6, derived from the C57BL/6 mouse genome, was used to construct a targeting vector through recombineering and site-specific recombinations by FRT and Cre. The BAC covers mm9 coordinates: 45,407,323 to 45,618,905 on chromosome 13, with the Idol gene near the middle. The bacterium carrying RP23-473O6 was cotransformed with the plasmid pBADgbaA, encoding arabinose-inducible expression of the lambda Red recombination protein. Exon 2 was "floxed" so as to create a frameshift mutation after Cre-mediated conditional deletion of the exon. Three sequential recombineering steps introduced Gateway attR1 and attR2 sites located upstream of exon 2 and a floxed kanamycin resistance (Kan^R) gene cassette downstream of exon 2 and trimmed the BAC to an approximately 10-kb fragment in a pBR-based plasmid flanked by attR3 and attR4 sites. The resulting clones were transformed into Cre-expressing bacteria to excise the floxed Kan^R cassette, leaving behind a single loxP site downstream of exon 2. A gene trap cassette (floxed β-galactosidase and neomycin (G418) markers with a 5′ lox71 site) was inserted at the attR1-to-attR2 Gateway sites, and the counterselection marker diphtheria toxin fragment A (DTA) was introduced into attR3 and attR4 sites by *in vitro* Gateway recombination. All modified junctions were verified by DNA sequencing, and a validated plasmid was selected for targeting in mouse embryonic stem (ES) cells. The plasmid was linearized with AsiSI and electroporated into 129/OlaHsd mouse ES cells using a GenePulser system (Bio-Rad). G418-resistant clones were picked and expanded, and targeted clones were identified by long-range PCR at both the 5′ and 3′ ends (data not shown). To generate ES cells homozygous for the targeted allele, targeted cells were cultured in medium containing high concentrations of G418 (1 mg/ml). Homozygous knockout cells were identified by PCR and quantitative reverse transcription-PCR (RT-PCR), and euploid clones, as judged by karyotyping, were selected for expansion.

Cell culture. Strain 129/OlaHsd mouse ES cells were cultured on gelatin-coated petri dishes in complete medium: Glasgow minimal essential medium (GMEM) (Sigma) supplemented with 2 mM L-glutamine (Invitrogen), 100 mM sodium pyruvate (Invitrogen), nonessential amino acids (1:100; Invitrogen), 10% fetal calf serum (FCS) (HyClone), leukemia inhibitory factor (LIF) (10^3 U/ml) (Chemicon), 0.1 mM β-mercaptoethanol, and 0.125 mg/ml G418. Cultures were maintained in a humidified chamber in 7% CO_2 at 37°C. To investigate the response to cholesterol depletion, ES cells were cultured in GMEM medium with 10% LPDS for the indicated times. In some experiments, GW3965, oxysterol, mevalonic acid, simvastatin, or PCSK9 was added to the medium. For detection of β-galactosidase, cells were fixed with glutaraldehyde for 15 min. After two washes, the cells were incubated in 5-bromo-4-chloro-3-indolyl-β-D-galactopyranoside (X-Gal) solution at 37°C overnight. Cells were rinsed, and digital images were captured.

LDL uptake assay. ES cells were incubated for 8 h in sterol-deficient medium to induce expression of the LDLR, and GW3965 was added to the medium for an additional 16 h. To measure LDL uptake, DiL-LDL (2.5 μg/ml) was added, followed by at 37°C for 6.5 h. The cells were washed with phosphate-buffered saline (PBS) containing 0.2% bovine serum albumin (BSA) and lysed in 500 μl radioimmunoprecipitation assay (RIPA) buffer supplemented with protease inhibitors and phenylmethylsulfonyl fluoride (PMSF). Lysates were collected and cleared by centrifugation, and aliquots (30 μl) were loaded into a 384-well plate. LDL uptake was measured with a Typhoon scanner (Amersham) at an excitation wavelength of 554 nm and an emission wavelength of 571 nm. Total cellular protein was measured using the Bradford protein assay, and fluorescence units were normalized to total protein.

RNA isolation and quantitative PCR. Total RNA was isolated from cells with Trizol reagent (Invitrogen). One microgram of total RNA was reverse transcribed with random hexamers with the iScript reverse transcription kit (Bio-Rad). Sybergreen (Diagenode) real-time quantitative PCR assays were performed with an Applied Biosystems 7900HT sequence detector. Results were normalized to 36B4.

Antibodies, immunoblots, and immunoprecipitations. Total cell lysates were prepared in RIPA buffer (150 mM NaCl, 1% NP-40, 0.1% sodium deoxycholate, 0.1% SDS, 100 mM Tris-HCl, pH 7.4) supplemented with protease inhibitors (Roche Molecular Biochemicals) and PMSF. Lysates were cleared by centrifugation at 4°C for 10 min at 10,000 × *g*. The protein concentration was determined with the bicinchoninic acid (BCA) protein assay (Pierce) with BSA as a reference. Samples (10 to 40 μg) were separated on NuPAGE Bis-Tris gels (Invitrogen) and transferred to nitrocellulose. Membranes were probed with the following antibodies: LDLR (1:1000; Cayman Chemical), ABCA1 (1:1000; Novus), actin (1:10,000; Sigma), HMGCS and FPPS (1:1000; a gift from Peter Edwards, University of California, Los Angeles), and TFRC (1:3,000; Zymed). Appropriate secondary horseradish peroxidase (HRP)-conjugated antibodies (Zymed) were used, and antibody binding was visualized by chemiluminescence. To immunoprecipitate LDLR, lysates were precleared by incubation with protein G-agarose beads (Santa Cruz) overnight. Subsequently, equal amounts of protein of cleared lysate were incubated with an LDLR-specific rabbit monoclonal antibody (1:30; Abcam) for 4 h before protein G-agarose beads were added for an additional 16 h. Subsequently, beads were washed 4× with RIPA buffer supplemented with protease inhibitors. All incubations and washes were done at 4°C with rotation. Proteins were eluted from the beads by boiling in 2× protein sample buffer for 5 min. Blots were quantified by densitometry with the ImageJ software program (version 1.42q; National Institutes of Health).

Metabolic labeling. ES cells were grown in GMEM supplemented with 10% LPDS for 16 h. Subsequently, cells were washed twice with PBS and pulsed for 30 min with Dulbecco's modified Eagle medium (DMEM) lacking methionine and cysteine (Sigma), supplemented with 200 μCi/well EasyTag L-[^{35}S]methionine protein-labeling mix (Perkin Elmer). Cells were then washed three times and chased in GMEM containing 10% LPDS, 100 μg/ml methionine, and 500 μg/ml cysteine for various time periods.

Surface biotinylation assay. The cell culture plates were rinsed twice with ice-cold PBS, pH 7.4, containing 0.02 mM $CaCl_2$ and 0.15 mM $MgCl_2$ (PBS-Ca-Mg). Cell surface proteins were biotinylated for 30 min with 0.25 mg/ml biotin (Sulfo-NHS-LC-Biotin; Pierce) diluted in PBS-Ca-Mg. Unbound biotin was quenched by three incubations (15 min at 4°C) with PBS-Ca-Mg containing 0.1 M glycine. Total protein fractions were extracted as described previously. Five hundred micrograms of total protein was precipitated with 60 μl of streptavidin-agarose beads (Pierce) overnight at 4°C by rotation. The beads were washed three times in cold RIPA buffer supplemented with protease inhibitors and two times in PBS-Ca-Mg. Biotinylated proteins (membrane proteins) were eluted from the beads by boiling in 2× sample buffer, separated on NuPAGE Bis-Tris

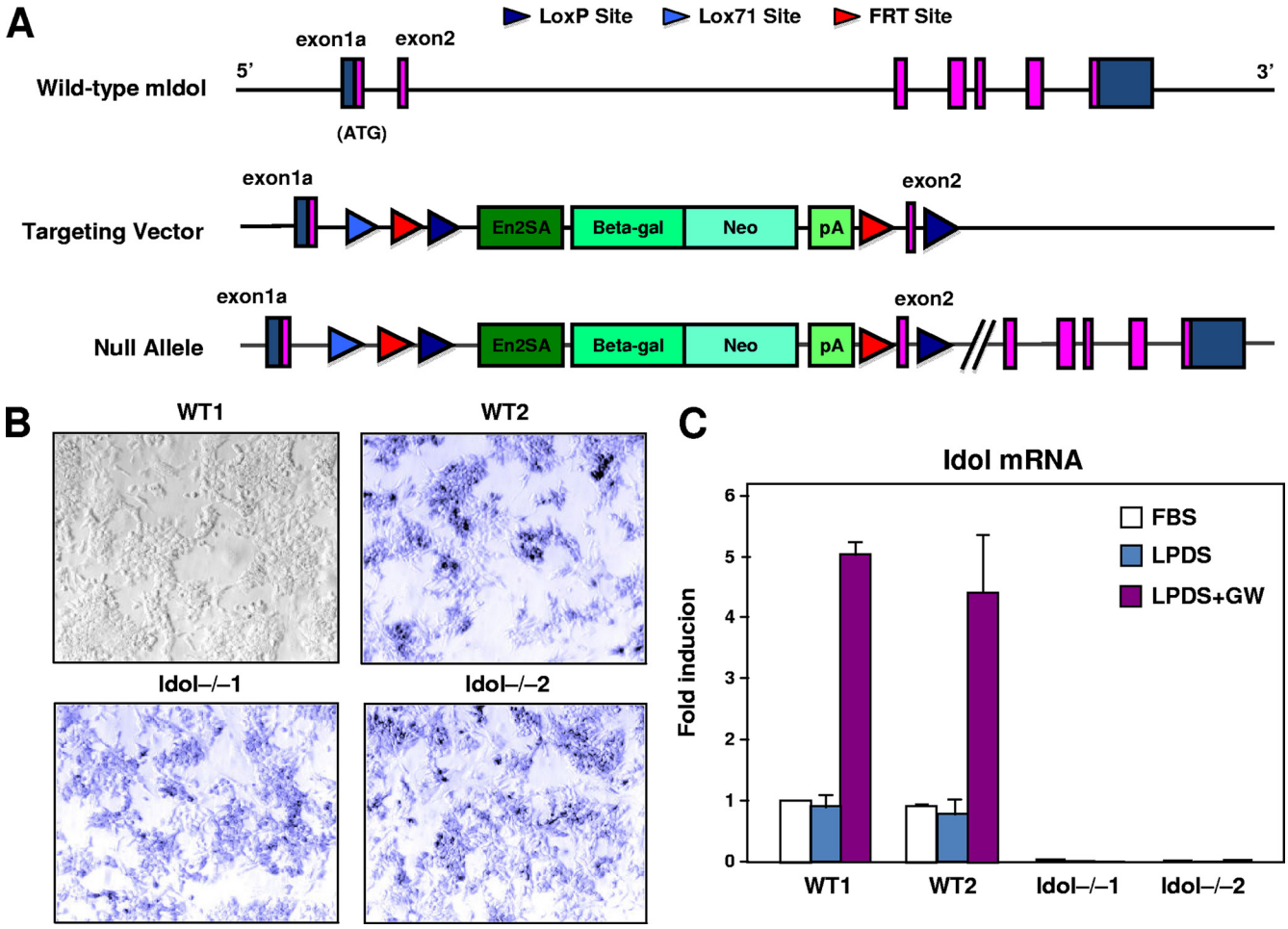

FIG. 1. Generation of Idol-deficient ES cells. (A) Schematic diagram of the Idol gene, which spans ~19 kb and contains 7 exons. The gene-trapping cassette (containing an *en2* splice acceptor site (En2SA) and a β-galactosidase-*neo* fusion [β*geo*]) was inserted into intron 1, and a downstream loxP site was inserted into intron 2. pA, polyadenylation signal; Beta-gal, β-galactosidase; Neo, neomycin phosphotransferase II. (B) β-Galactosidase was expressed in ES cell lines carrying a ßgeo gene trap cassette (WT2, Idol−/−1, and Idol−/−2), as judged by staining with X-Gal. WT1, the parental ES cell line, is shown for comparison. WT2 is targeted for the *Tle3* gene. LPD, LPDS-containing medium. (C) Idol gene expression was determined in ES cells ($n = 5$) cultured in 10% FBS or LPDS-containing medium for 8 h and then treated with the LXR agonist GW (1 μM) for 16 h. The WT1 FBS point was assigned a value of 1, and data are plotted as fold induction over this level. Shown are means ± SD.

gels (Invitrogen), and transferred to nitrocellulose as described previously. Blots were quantified by densitometry using the ImageJ software program.

Degradation assay. ES cells were grown in GMEM medium supplemented with 10% LPDS for 16 h. Cells were then cooled rapidly to 4°C, and the surfaces of the cells were biotinylated and quenched as described for the surface biotinylation assay. Prewarmed medium containing 10% LPDS was added for the indicated times at 37°C. The cells were solubilized in RIPA, and biotinylated LDLR proteins were separated from nonbiotinylated proteins with avidin beads. LDLR bands were scanned, and the immunoblots were quantified with the ImageJ software program.

Statistical analysis. Real-time PCR data and results of LDL uptake assays were expressed as means ± standard deviations. Statistical analyses were performed with one-way analysis-of-variance tests with the GraphPad Prism program, version 4.0 (GraphPad Software).

RESULTS

Generation of Idol-deficient embryonic stem cells. To determine the function of Idol in cellular cholesterol metabolism, we generated Idol-deficient ES cells. The targeting vector employed a floxed gene trap cassette consisting of an *en2* splice acceptor site, a β-galactosidase-*neo* marker, and an upstream Lox71 site (Fig. 1A). The gene trap cassette was inserted into intron 1, and an additional loxP site was inserted into intron 2. The targeting vector DNA was electroporated into ES cells, and two Idol knockout ES cell lines were established (Idol−/−1 and Idol−/−2). As controls, we used the parental ES cell line (WT1) and an ES cell line carrying a homozygous mutation in another gene (*Tle3*) unrelated to cholesterol metabolism (WT2). As expected, Idol-null ES cells as well as the targeted WT2 cells were positive for β-galactosidase expression (Fig. 1B). To evaluate Idol mRNA expression, we performed real-time PCR. Idol mRNA was expressed and responsive to the LXR agonist (GW3965) in both WT ES cell lines but was undetectable in Idol-null clones (Fig. 1C). Unfortunately, there are currently no antibodies available capable of detecting the very low levels of endogenous Idol protein.

Altered LDLR protein levels in Idol-deficient cells. We initially used Idol-deficient ES cells to test our prediction that

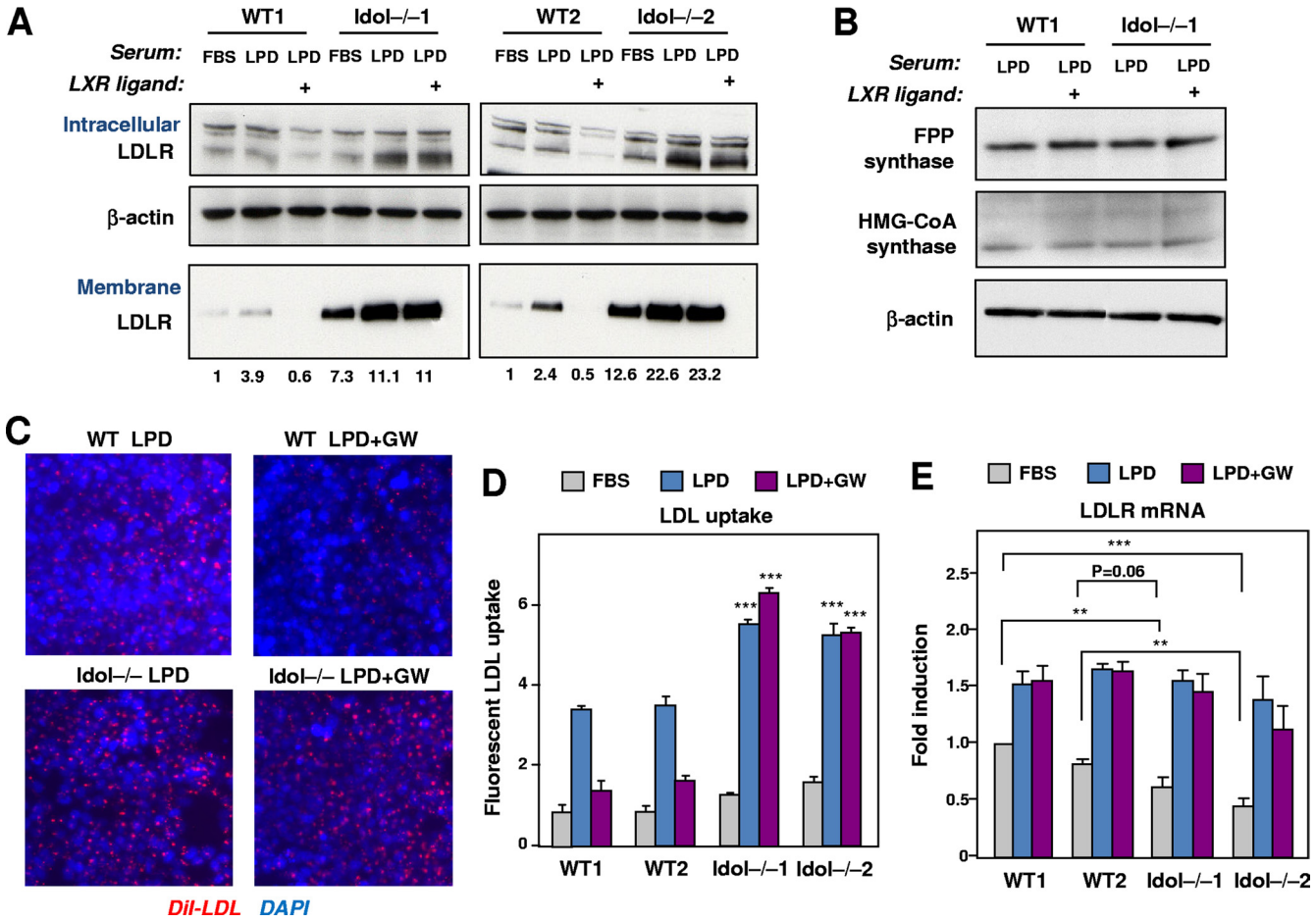

FIG. 2. Altered LDLR protein levels in Idol-deficient cells. (A) ES cells were cultured in 10% LPDS medium for 8 h and then treated with dimethyl sulfoxide (DMSO) or the LXR agonist GW (1 μM) for 16 h. Expression of LDLR was analyzed in membranes and total cell extracts. Membrane proteins were labeled with biotin as described in Materials and Methods. Endogenous β-actin was used as a loading control. Quantification of membrane LDLR levels by densitometry is shown below the images. Blots are representative of 3 independent experiments. (B) Immunoblot analysis of FPPS and HMGCoAS from ES cells grown in 10% LPDS medium for 8 h and then treated with DMSO or the LXR agonist GW (1 μM) for 16 h. β-Actin was used as a loading control. Data are representative of two independent experiments. (C) Dil-LDL uptake (red staining) in ES cells grown in LPDS medium for 8 h and subsequently treated with DMSO or the LXR ligand GW3965 (1 μM) for 16 h. Nuclei were counterstained with 4′,6-diamidino-2-phenylindole (DAPI) (blue). (D) Quantification of LDL uptake (mean ± standard deviation for three measurements). ***, $P < 0.001$ for the comparison of WT and Idol-null ES cells. (E) LDLR gene expression was determined in ES cells ($n = 5$) cultured in 10% LPDS medium for 8 h and then treated with DMSO or the LXR agonist GW (1 μM) for 16 h. Means ± SD are shown. The WT1 FBS point was assigned a value of 1, and data are plotted as fold induction over this level. **, $P < 0.01$; ***, $P < 0.001$.

Idol expression was a determinant of LDLR protein levels. We examined LDLR expression in response to changes in the sterol content of the medium and in response to an LXR agonist. Both intracellular and plasma membrane LDLR protein levels were measured. To examine plasma membrane LDLR protein levels, we employed a biotin-labeling strategy as described in Materials and Methods. As expected, switching WT ES cells from 10% FBS to 10% lipoprotein-deficient serum (LPDS) increased LDLR protein levels (Fig. 2A). Remarkably, treatment with GW3965 eliminated membrane LDLR protein levels. In contrast, Idol$^{-/-}$ ES cells exhibited two differences from WT cells. First, we detected more LDLR on the membrane, both in the basal state and after stimulation with LPDS medium. Second, the response of LDLR to the LXR agonist was abolished in Idol-deficient cells. Intracellular LDLR protein levels paralleled surface levels, although the magnitude of regulation was more modest (Fig. 2A). In contrast to the case with LDLR, LXR activation had no effect on protein levels of farnesyl diphosphate (FPP) synthase or 3-hydroxy-3-methylglutaryl-coenzyme A (HMGCoA) synthase in WT or Idol$^{-/-}$ cells (Fig. 2B). These data demonstrate that the genetic absence of Idol increases both basal and inducible expression of the membrane LDLR protein and that Idol is required for the effect of LXR on the LDLR pathway.

To investigate the consequences of LDLR upregulation in Idol$^{-/-}$ cells, we measured the uptake of fluorescently labeled LDL by cells. In WT ES cells, LDL uptake was increased when the FBS medium was changed to the LPDS medium and was reduced when the LXR ligand was added to the medium (Fig. 2C and D). However, in Idol-null cells, we observed increased LDL uptake in response to low-cholesterol conditions, and the effect of the LXR agonist was absent. These results are con-

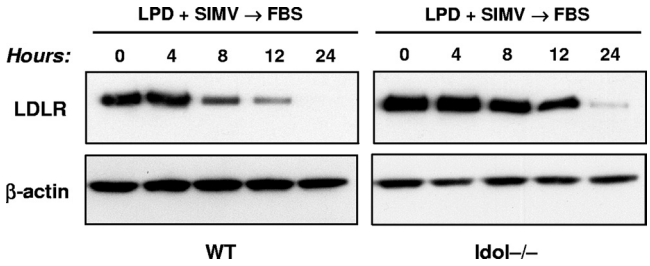

FIG. 3. Loss of Idol expression diminishes sterol-dependent downregulation of the LDLR. ES cells were grown in sterol depletion medium (10% LPDS with 5 μM simvastatin and 100 μM mevalonic acid) for 16 h, and the medium was then changed to lipoprotein-rich FBS medium (10% FBS) for the indicated times. The levels of LDLR and β-actin were determined by immunoblotting. Similar results were obtained in 3 independent experiments.

sistent with our results on LDLR protein expression (Fig. 2A). Interestingly, basal levels of LDLR expression were slightly lower in Idol$^{-/-}$ cells than in WT cells, suggesting possible reduced activity of the SREBP pathway (Fig. 2E).

Loss of Idol expression impairs sterol-dependent downregulation of LDLR. We next examined the ability of Idol to mediate the cellular response to lipoprotein-rich serum. Cells were sterol starved by culture in LPDS medium containing simvastatin and then refed with FBS medium. In WT ES cells, FBS suppressed the LDLR protein faster than in Idol$^{-/-}$ cells (Fig. 3).

We next addressed the role of Idol in mediating the inhibitory effects of oxysterols on the LDLR pathway. It is well established that oxysterols inhibit SREBP-2 processing and thereby inhibit LDLR mRNA expression (1, 26). At the same time, oxysterols are ligands for LXR and therefore stimulate Idol expression (10, 27). We tested the effects of two oxysterols in our model: 22(*R*)-hydroxycholesterol, a potent LXR ligand with weak activity for the SREBP-2 pathway; and 25-hydroxycholesterol, a weak LXR agonist and potent inhibitor of SREBP-2 processing (11). WT and Idol$^{-/-}$ ES cells were incubated in the presence of oxysterols (2.5 μM). At various intervals, the cells were biotinylated and membrane proteins were extracted and analyzed by immunoblotting. Figure 4 shows the time course of sterol-mediated suppression of plasma membrane LDLR. In WT cells (where both the SREBP-2 and Idol pathways are functional), treatment with 22(*R*)-hydroxycholesterol rapidly decreased membrane LDLR levels (>70% reduction in 4 h). At least 8 h were required to produce a 70% reduction in LDLR levels in Idol$^{-/-}$ cells (Fig. 4A and B). The kinetics of LDLR suppression were also different in WT and Idol-null cells after treatment with 25-hydroxycholesterol (Fig. 4C and D). 25-Hydroxycholesterol was a more effective suppressor of LDLR expression in Idol-deficient cells than 22(*R*)-hydroxycholesterol, consistent with the fact that 25-hydroxycholesterol is a more effective inhibitor of SREBP-2 cleavage. Importantly, the effects of sterols were specific to the LDLR, since there were no significant changes in levels of the transferrin receptor. Compared with oxysterols, the effects of a synthetic LXR agonist on LDLR protein levels were more rapid and more potent, consistent with its greater ability to activate the Idol pathway (Fig. 4E and F). Collectively, the data in Fig. 3 and 4 show that the endogenous Idol pathway is an important contributor to feedback inhibition of the LDLR by sterols.

Idol can affect LDLR before and after it has reached the plasma membrane. We sought to address where in the itinerary of the LDLR it is targeted by Idol. One possibility is that Idol targets LDLR either when it is present on the membrane or after it is internalized by endocytosis. To test these possibilities, we adapted our biotin-labeling strategy to monitor the turnover of the membrane LDLR. Plasma membrane proteins were biotinylated in adherent ES cells at 0°C. After a wash, the cells were warmed to 37°C to induce internalization of LDLR. This approach allowed us to monitor the turnover of LDLR after its appearance on the plasma membrane. The degradation of LDLR on the membrane was more rapid in WT ES cells than in Idol$^{-/-}$ cells (Fig. 5A). This difference was confirmed by densitometric analysis (Fig. 5B). Thus, Idol can target the LDLR for degradation after it has reached the membrane. Furthermore, in the absence of Idol, postmembrane degradation of the LDLR is reduced.

To investigate if Idol also targets the LDLR before reaching the plasma membrane, we analyzed the effect of an LXR agonist on newly synthesized LDLR in WT and Idol-deficient ES cells. Cells were first treated with 25-hydroxycholesterol to decrease basal levels of the LDLR protein. Subsequently, cells were incubated in lipoprotein-deficient medium to induce new LDLR synthesis. The effect of LXR agonist treatment on the appearance of new LDLR protein was then analyzed. Treatment with GW3965 effectively prevented the appearance of new LDLR protein in WT cells but not Idol$^{-/-}$ cells (Fig. 5C). Cumulatively, the data shown in Fig. 5 indicate that Idol can affect levels of the LDLR protein both before and after it reaches the plasma membrane.

LDLR half-life in Idol-null cells. The data presented to this point support the hypothesis that Idol degrades the LDLR. To provide direct evidence for this concept, we performed pulse-chase metabolic labeling studies. ES cells were labeled for 30 min with [^{35}S]methionine and then chased for the indicated times in medium containing unlabeled methionine (Fig. 6). The LDLR was immunoprecipitated and analyzed by SDS-PAGE. The amount of labeled LDLR remaining at each time point was quantified by densitometry. Remarkably, the loss of Idol expression dramatically increased the half-life of the LDLR protein. The LDLR in Idol$^{-/-}$ ES cells was stable, whereas in WT ES cells it was turned over rapidly. The half-life of the LDL receptor in WT ES cells was estimated to be ~4 h, compared with >8 h in Idol$^{-/-}$ cells.

Relationship of Idol to the statin and PCSK9 pathways. The statin drugs act by inhibiting cholesterol biosynthesis, causing SREBP-2-dependent upregulation of the LDLR. We examined the relationship between the Idol pathway and the "statin pathway." Treatment of WT ES cells with simvastatin in LPDS medium increased LDLR expression by almost 2-fold (Fig. 7). Interestingly, simvastatin maintained its ability to increase LDLR protein levels in Idol$^{-/-}$ cells, even though baseline LDLR levels were already very high in Idol$^{-/-}$ cells. As expected, an LXR agonist failed to repress LDLR protein levels in Idol$^{-/-}$ cells whether simvastatin was present or not. These results indicate that the effects of statins and the Idol pathway on LDLR protein levels are additive.

LDLR protein levels are also regulated by the PCSK9, a

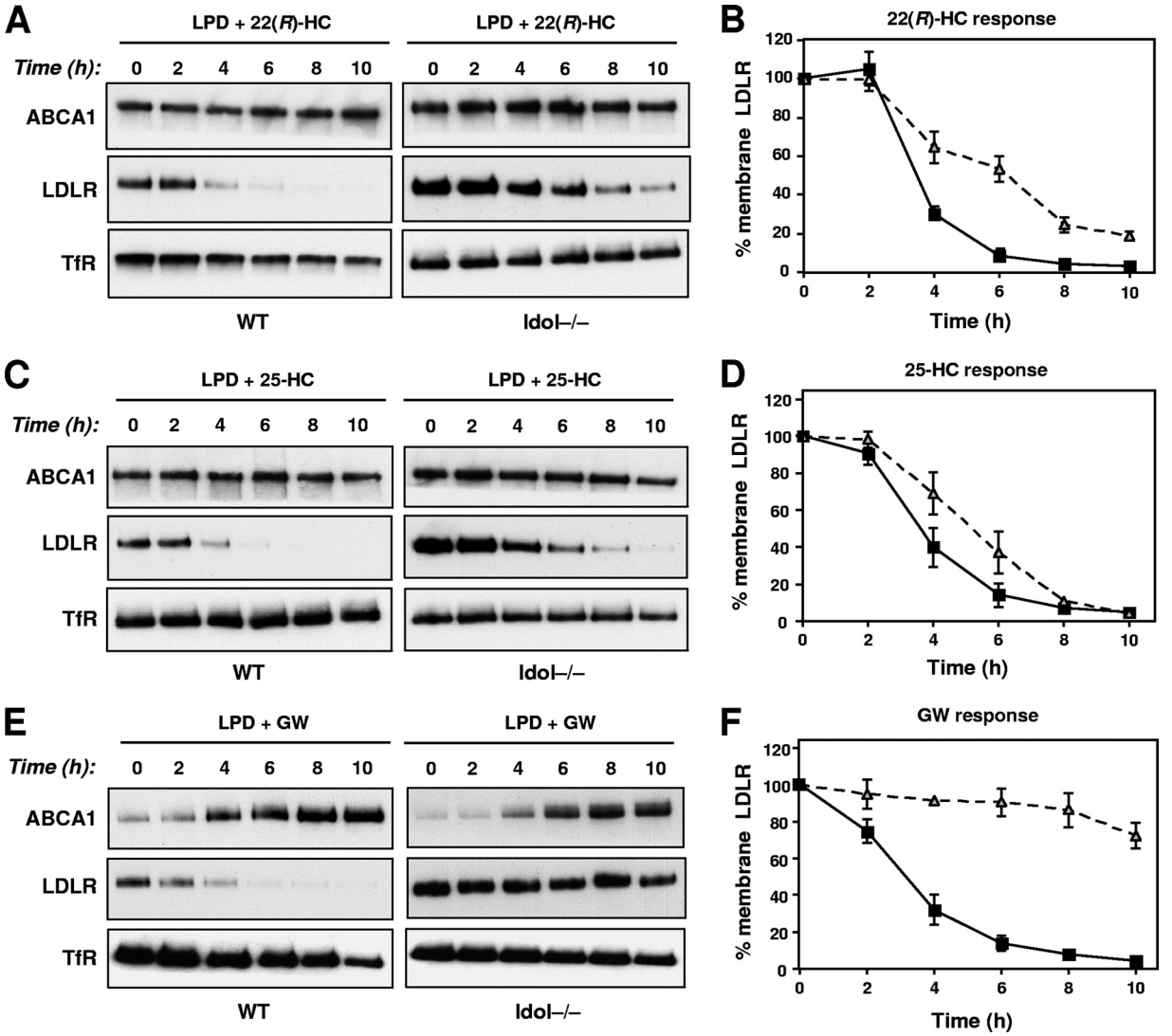

FIG. 4. Oxysterol-dependent downregulation of the LDLR is impaired by the loss of Idol expression. (A, C, and E) ES cells were cultured in 10% LPDS medium for 16 h and then treated with 22(*R*)-hydroxycholesterol (2.5 μM), 25-hydroxycholesterol (2.5 μM), or GW3965 (1 μM) for the indicated times. Membrane lysates were analyzed by immunoblotting. Endogenous transferrin receptor (TfR) levels were also measured as a control. Blots are representative of 3 independent experiments. (B, D, and F) Quantitative analysis of three independent replicates of the blots shown in panels A, C, and E. Results are expressed as a percentage of the amount of receptor at time zero.

secreted protein that interacts with the epidermal growth factor (EGF)-like repeat A (EGF-A) of the LDLR and enters the cell through clathrin/ARH-mediated endocytosis (13, 16, 18). We considered the possibility that Idol might act downstream of the PCSK pathway, possibly mediating LDLR degradation after PCSK9-dependent internalization. To test this idea, we treated WT and Idol$^{-/-}$ ES cells with purified PCSK9 or the BSA control. Analysis of total cell lysates by immunoblotting revealed that PCSK9 was highly effective in reducing LDLR protein levels in both WT and Idol$^{-/-}$ ES cells (Fig. 8A). Interestingly, we were unable to detect expression of the endogenous PCSK9 protein in ES cells. We also analyzed the effect of PCSK9 on plasma membrane proteins using our biotin-labeling strategy. Again, in contrast to the LXR agonist, PCSK9 was highly effective in reducing LDLR protein levels in both WT and Idol$^{-/-}$ ES cell (Fig. 8B). The magnitude of the effect of PCSK9 in WT ES cells was comparable to the effect of the synthetic LXR agonist. These results indicate that PCSK9 and Idol reduce LDLR protein levels by distinct mechanisms.

DISCUSSION

The LDLR is responsible for transporting cholesterol-containing lipoprotein particles (LDL or VLDL) from the plasma into cells. Upon LDL binding, the receptor-ligand complex is internalized via clathrin-mediated endocytosis. In endosomes, the receptor dissociates from its ligand at acidic pH and then recycles back to the cell surface. The lipoprotein particles proceed to lysosomes, where the cholesterol esters are hydrolyzed to liberate free cholesterol (2–4). LDLR protein levels are highly regulated to avoid the cytotoxicity associated with excess free cholesterol. It is therefore not surprising that com-

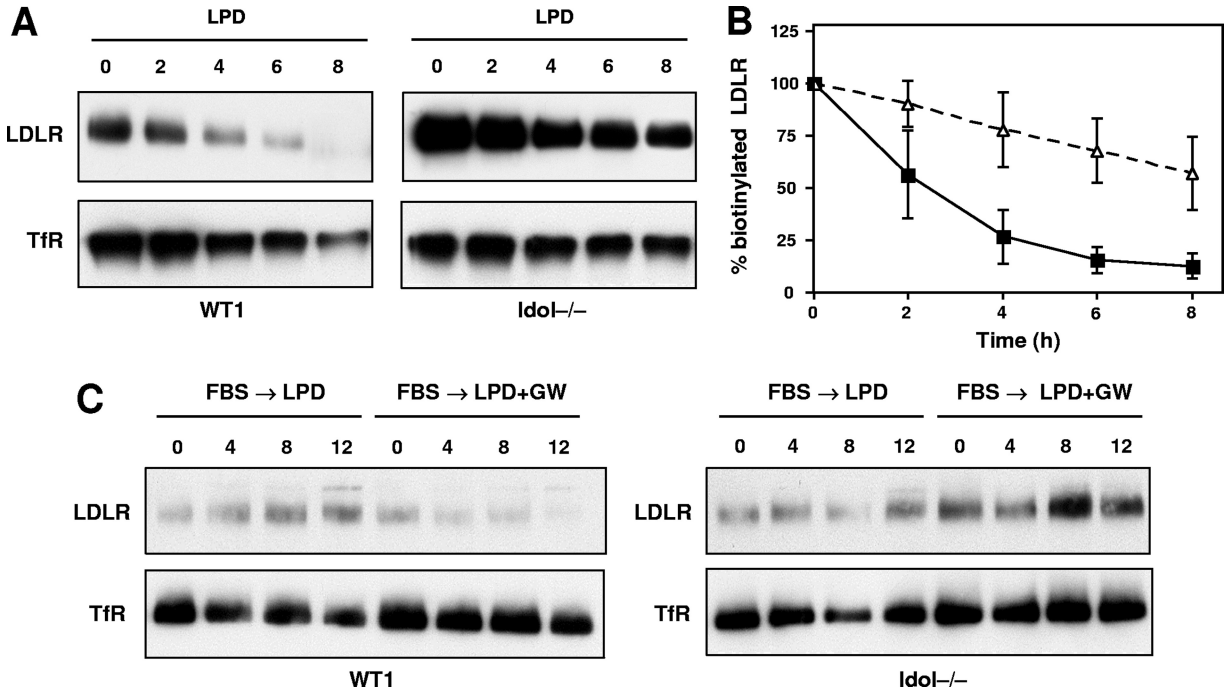

FIG. 5. Idol affects LDLR expression at the plasma membrane. (A) Cells grown in lipoprotein-deficient medium were surface labeled with Sulfo-NHS-LC-Biotin for 30 min at 4°C. The cells were then incubated at 37°C for the indicated times to allow internalization. Biotinylated proteins were then analyzed as described in Materials and Methods. LDLR and TFRC immunoblots are shown. Qualitatively similar results were obtained in 3 independent experiments. (B) Quantitative analysis of three independent replicates of the blot shown in panel A. (C) Idol can affect LDLR before it reaches the plasma membrane. ES cells were pretreated with 25-hydroxycholesterol (2.5 μM) for 16 h and subsequently grown in LPDS containing either DMSO or GW for the indicated time points. Surface proteins were collected and analyzed as described in Materials and Methods. Qualitatively similar results were obtained in 2 independent experiments.

plementary mechanisms have evolved to maintain cholesterol homeostasis. These strategies include the SREBP-2 pathway, which controls LDLR gene expression (7), and the LXR-Idol pathway (27), which, together with PCSK9 (5, 15, 28), is involved in LDLR degradation.

In the current study, we characterized ES cells carrying a null mutation in the Idol gene. Genetic absence of Idol has unmistakable consequences for the regulation of endogenous LDLR protein levels, strongly supporting hypotheses proposed in our earlier studies (27). Our data demonstrate that Idol is absolutely required for the effect of LXR on the LDLR pathway. A highly efficacious synthetic LXR agonist did not affect LDLR protein expression or LDL uptake in Idol$^{-/-}$ cells. We also found that basal LDLR protein levels in ES cells lacking Idol are much higher than in WT cells despite their having lower LDLR mRNA levels. Furthermore, the increased number of LDLR molecules on the plasma membrane translated into an increased capacity for LDL uptake. These results are reminiscent of previous observations of primary hepatocytes from Pcsk9$^{-/-}$ mice (20). Interestingly, increased LDLR ex-

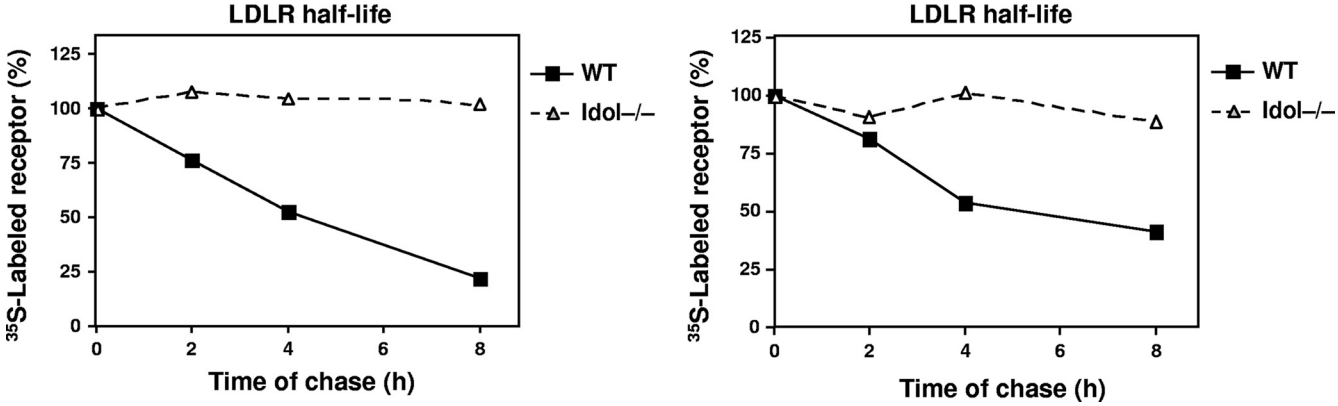

FIG. 6. Loss of Idol increases LDLR half-life in ES cells. Cells were pulse-labeled with [^{35}S]methionine for 30 min and chased for times indicated. Samples were immunoprecipitated at the indicated time points, and the LDLR protein was measured as described in Materials and Methods. Results of two independent experiments are shown.

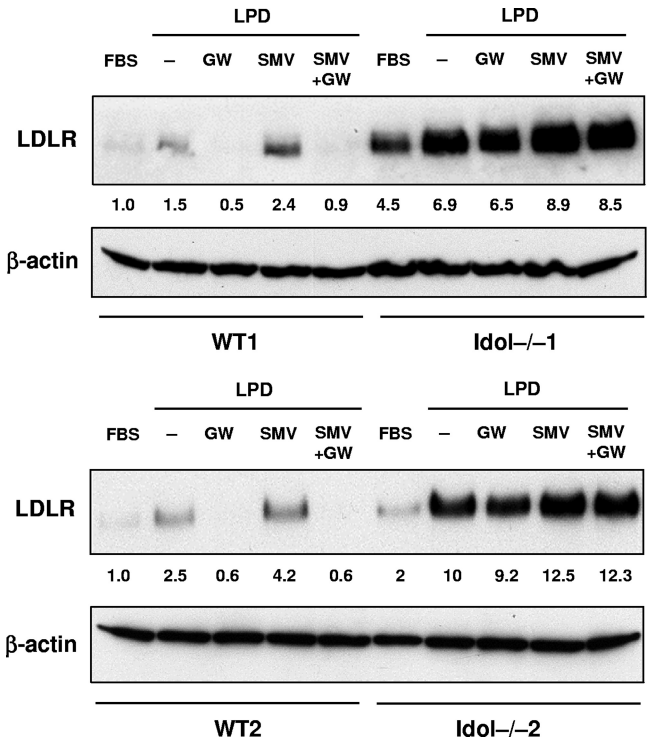

FIG. 7. The Idol pathway is independent of, and additive with, statins and PCSK9. ES cells were grown in 10% LPDS medium or in sterol depletion medium (LPDS with 5 μM simvastatin [SMV] and 100 μM mevalonic acid) for 8 h and then treated with DMSO or the LXR agonist GW (1 μM) for 16 h. Membranes and total cell lysates were prepared, and immunoblots for LDLR and β-actin were performed. Quantification of LDLR expression by densitometry is shown below each lane.

pression in Idol$^{-/-}$ cells appears to provoke a compensatory response from the SREBP-2 pathway, since LDLR mRNA expression is modestly but consistently reduced in Idol$^{-/-}$ cells cultured in sterol-rich medium.

Our studies clarify the complementary roles of the Idol and SREBP-2 pathways in feedback control of LDLR protein levels by sterols. One advantage of the Idol pathway may be the capacity for a rapid response to changing sterol levels. We show that activation of LXR leads to a dramatic reduction in plasma membrane LDLR protein within 2 h. Although cells lacking Idol can still downregulate LDLR expression through the SREBP-2 pathway, the kinetics are slower, supporting the hypothesis that Idol may be particularly important in the early response to sterols. It is also interesting that oxysterols exhibit different effects on the SREBP-2 and LXR-Idol pathways depending on their relative capacities to inhibit SREBP processing and activate LXRs.

Our studies also demonstrated that Idol is an important determinant of the half-life of the LDLR protein, at least in certain cell types. In ES cells, the LDLR protein was relatively short lived, similar to findings in J774 cells (23). Moreover, since the LDLR half-life was prolonged in Idol$^{-/-}$ cells, it appears that the basal LDLR expression levels in ES cells depend on Idol. Similarly, plasma membrane levels of LDLR decayed more rapidly in WT cells than in Idol$^{-/-}$ cells.

Characterization of Idol-deficient cells has also provided insights into to the functional relationship between the PCSK9 and Idol pathways. PCSK9 and Idol share the same protein substrates, suggesting that their biological functions may be complementary (9, 19, 22, 27). While PCSK9 induces LDLR degradation primarily by binding the extracellular domain (15–24), Idol works intracellularly, both before and after the receptor reaches the membrane. We initially suspected that Idol would promote LDLR degradation downstream of PCSK9-mediated internalization and therefore be dependent on the action of PCSK9. However, our studies clearly show that PCSK9 is still able to induce LDLR degradation in Idol$^{-/-}$ cells, suggesting that Idol and PCSK9 act in complementary but independent pathways. Similarly, the effects of statins and Idol on LDLR expression are also additive and independent. Statins exert their cholesterol-lowering effects by inhibiting cholesterol biosynthesis and by the SREBP-dependent upregulation of LDLR transcription (14, 17). In ES cells, inactivating Idol stabilizes the LDLR protein levels induced by statins, enhancing the pharmacological effect.

Collectively, our data suggest that the LXR-Idol pathway may provide a third mechanism for pharmacologic manipulation of cellular LDLR expression. However, more research will be needed to determine the relative importance of various sterol regulatory mechanisms in specific cell types. This study

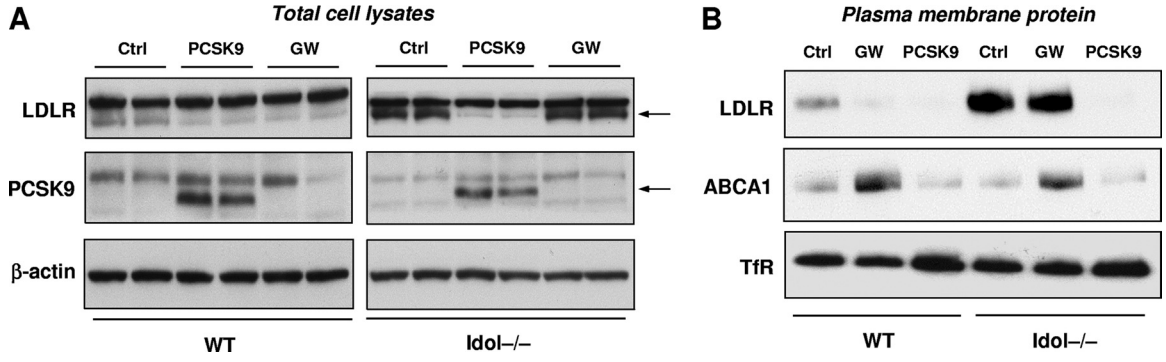

FIG. 8. PCSK9 promotes LDLR degradation in the absence of Idol. (A) Immunoblot analysis of total cell lysates from ES cells cultured in 10% LPDS medium for 8 h and then treated with BSA or the LXR agonist GW (1 μM) or BSA (Ctrl) or purified PCSK9 (5 μg/ml) for 24 h. Arrows indicate specific LDLR and PCSK9 bands. (B) Immunoblot analysis of plasma membrane protein lysates from ES cells cultured in 10% LPDS medium for 8 h and then treated with BSA or the LXR agonist GW (1 μM) or BSA (Ctrl) or purified PCSK9 (5 μg/ml) for 24 h.

has utilized ES cells as a model system, but in the future it will be important to test the effect of Idol deletion in additional cell types, such as fibroblasts, hepatocytes, and macrophages. Preliminary data indicate that homozygous Idol$^{-/-}$ mice are viable and will be useful tools to address systemic and cell type-specific Idol effects. An important goal of future research will be to investigate the consequence of Idol action for hepatic and peripheral LDLR expression and to test the effect of Idol inhibition on cholesterol homeostasis *in vivo*.

ACKNOWLEDGMENTS

We thank Peter Edwards and Karen Reue for helpful discussions.

P.T. is an investigator of the Howard Hughes Medical Institute. E.S. was partially supported by a fellowship from the Dipartimento di Scienze Farmacologiche, Università degli Studi di Milano. This work was also supported by NIH grants HL090553, HL066088, HL030568, and DK063491.

We have no conflict of interest to disclose.

REFERENCES

1. **Brown, A. J., L. Sun, J. D. Feramisco, M. S. Brown, and J. L. Goldstein.** 2002. Cholesterol addition to ER membranes alters conformation of SCAP, the SREBP escort protein that regulates cholesterol metabolism. Mol. Cell **10:**237–245.
2. **Brown, M. S., and J. L. Goldstein.** 1976. Receptor-mediated control of cholesterol metabolism. Science **191:**150–154.
3. **Brown, M. S., and J. L. Goldstein.** 1997. The SREBP pathway: regulation of cholesterol metabolism by proteolysis of a membrane-bound transcription factor. Cell **89:**331–340.
4. **Brown, M. S., J. Herz, and J. L. Goldstein.** 1997. LDL-receptor structure. Calcium cages, acid baths and recycling receptors. Nature **388:**629–630.
5. **Cameron, J., et al.** 2008. Investigations on the evolutionary conservation of PCSK9 reveal a functionally important protrusion. FEBS J. **275:**4121–4133.
6. **Dai, X. Y., et al.** 2008. The effect of T0901317 on ATP-binding cassette transporter A1 and Niemann-Pick type C1 in apoE−/− mice. J. Cardiovasc. Pharmacol. **51:**467–475.
7. **Goldstein, J. L., and M. S. Brown.** 1990. Regulation of the mevalonate pathway. Nature **343:**425–430.
8. **Grefhorst, A., M. C. McNutt, T. A. Lagace, and J. D. Horton.** 2008. Plasma PCSK9 preferentially reduces liver LDL receptors in mice. J. Lipid Res. **49:**1303–1311.
9. **Hong, C., et al.** 2010. The E3 ubiquitin ligase IDOL induces the degradation of the low density lipoprotein receptor family members VLDLR and ApoER2. J. Biol. Chem. **285:**19720–19726.
10. **Janowski, B. A., et al.** 1999. Structural requirements of ligands for the oxysterol liver X receptors LXRalpha and LXRbeta. Proc. Natl. Acad. Sci. U. S. A. **96:**266–271.
11. **Janowski, B. A., P. J. Willy, T. R. Devi, J. R. Falk, and D. J. Mangelsdorf.** 1996. An oxysterol signalling pathway mediated by the nuclear receptor LXRα. Nature **383:**728–731.
12. **Laffitte, B. A., et al.** 2001. LXRs control lipid-inducible expression of the apolipoprotein E gene in macrophages and adipocytes. Proc. Natl. Acad. Sci. U. S. A. **98:**507–512.
13. **Lagace, T. A., et al.** 2006. Secreted PCSK9 decreases the number of LDL receptors in hepatocytes and in livers of parabiotic mice. J. Clin. Invest. **116:**2995–3005.
14. **Liao, J. K., and U. Laufs.** 2005. Pleiotropic effects of statins. Annu. Rev. Pharmacol. Toxicol. **45:**89–118.
15. **Lopez, D.** 2008. PCSK9: an enigmatic protease. Biochim. Biophys. Acta **1781:**184–191.
16. **McNutt, M. C., et al.** 2009. Antagonism of secreted PCSK9 increases low density lipoprotein receptor expression in HepG2 cells. J. Biol. Chem. **284:**10561–10570.
17. **Miida, T., S. Hirayama, and Y. Nakamura.** 2004. Cholesterol-independent effects of statins and new therapeutic targets: ischemic stroke and dementia. J. Atheroscler. Thromb. **11:**253–264.
18. **Nassoury, N., et al.** 2007. The cellular trafficking of the secretory proprotein convertase PCSK9 and its dependence on the LDLR. Traffic **8:**718–732.
19. **Poirier, S., et al.** 2008. The proprotein convertase PCSK9 induces the degradation of low density lipoprotein receptor (LDLR) and its closest family members VLDLR and ApoER2. J. Biol. Chem. **283:**2363–2372.
20. **Poirier, S., et al.** 2009. Dissection of the endogenous cellular pathways of PCSK9-induced low density lipoprotein receptor degradation: evidence for an intracellular route. J. Biol. Chem. **284:**28856–28864.
21. **Repa, J. J., et al.** 2000. Regulation of absorption and ABC1-mediated efflux of cholesterol by RXR heterodimers. Science **289:**1524–1529.
22. **Shan, L., et al.** 2008. PCSK9 binds to multiple receptors and can be functionally inhibited by an EGF-A peptide. Biochem. Biophys. Res. Commun. **375:**69–73.
23. **Shite, S., T. Seguchi, T. Shimada, M. Ono, and M. Kuwano.** 1990. Rapid turnover of low-density lipoprotein receptor by a non-lysosomal pathway in mouse macrophage J774 cells and inhibitory effect of brefeldin A. Eur. J. Biochem. **191:**491–497.
24. **Steinberg, D., and J. L. Witztum.** 2009. Inhibition of PCSK9: a powerful weapon for achieving ideal LDL cholesterol levels. Proc. Natl. Acad. Sci. U. S. A. **106:**9546–9547.
25. **Venkateswaran, A., et al.** 2000. Control of cellular cholesterol efflux by the nuclear oxysterol receptor LXR alpha. Proc. Natl. Acad. Sci. U. S. A. **97:**12097–12102.
26. **Yamamoto, T., et al.** 1984. The human LDL receptor: a cysteine-rich protein with multiple Alu sequences in its mRNA. Cell **39:**27–38.
27. **Zelcer, N., C. Hong, R. Boyadjian, and P. Tontonoz.** 2009. LXR regulates cholesterol uptake through Idol-dependent ubiquitination of the LDL receptor. Science **325:**100–104.
28. **Zhang, D. W., et al.** 2007. Binding of proprotein convertase subtilisin/kexin type 9 to epidermal growth factor-like repeat A of low density lipoprotein receptor decreases receptor recycling and increases degradation. J. Biol. Chem. **282:**18602–18612.